ORIGINAL ARTICLE

BCPT
Basic & Clinical Pharmacology & Toxicology

Enhanced agonist residence time, internalization rate and signalling of the GIP receptor variant [E354Q] facilitate receptor desensitization and long-term impairment of the GIP system

Maria Buur Nordskov Gabe[1] | **Wijnand J. C. van der Velden**[1] | **Sarina Gadgaard**[1] |
Florent Xavier Smit[1] | **Bolette Hartmann**[1,2] | **Hans Bräuner-Osborne**[3] |
Mette Marie Rosenkilde[1]

[1]Department of Biomedical Sciences, Faculty of Health and Medical Sciences, University of Copenhagen, Copenhagen, Denmark

[2]Novo Nordisk Foundation Center for Basic Metabolic Research, University of Copenhagen, Copenhagen, Denmark

[3]Department of Drug Design and Pharmacology, Faculty of Health and Medical Sciences, University of Copenhagen, Copenhagen, Denmark

Correspondence
Mette Marie Rosenkilde, Department of Biomedical Sciences, Faculty of Health and Medical Sciences, University of Copenhagen, Copenhagen, Denmark.
Email: rosenkilde@sund.ku.dk

Funding information
Carlsberg Foundation

Abstract

In patients with type 2 diabetes mellitus (T2DM), the insulinotropic action of the GIP system is desensitized, whereas this is not the case for the GLP-1 system. This has raised an interesting discussion of whether GIP agonists or antagonists are most suitable for future treatment of T2DM together with GLP-1-based therapies. Homozygous carriers of the GIP receptor (GIPR) variant, [E354Q], display lower bone mineral density, increased bone fracture risk and slightly increased blood glucose. Here, we present an in-depth molecular pharmacological phenotyping of GIPR-[E354Q]. In silico modelling suggested similar interaction of the endogenous agonist GIP(1-42) to [E354Q] as to GIPR wt. This was supported by homologous competition binding in COS-7 cells revealing GIPR wt-like affinities of GIP(1-42) with K_d values of ~2 nmol/L and wt-like agonist association rates (K_{on}). In contrast, the dissociation rates (K_{off}) were slower, resulting in 25% higher agonist residence time for GIPR-[E354Q]. Moreover, in $G_{\alpha s}$ signalling (cAMP production) GIP(1-42) was ~2-fold more potent and more efficacious on GIPR-[E354Q] compared to wt with 17.5% higher basal activity. No difference from GIPR wt was found in the recruitment of β-arrestin 2, whereas the agonist-induced internalization rate was 2.1- to 2.3-fold faster for [E354Q]. Together with the previously described impaired recycling of [E354Q], our findings with enhanced signalling and internalization rate possibly explained by an altered ligand-binding kinetics will lead to receptor desensitization and down-regulation. This could explain the long-term functional impairment of the GIP system in bone metabolism and blood sugar maintenance for [E354Q] carriers and may shed light on the desensitization of the insulinotropic action of GIP in patients with T2DM.

KEYWORDS
GIP receptor, GIPR-[E354Q], internalization, signalling

1 | INTRODUCTION

Glucose-dependent insulinotropic polypeptide (GIP) is a 42 amino acid long peptide hormone that is secreted from enteroendocrine K cells located in the proximal part of the small intestine in response to food intake.[1] As an incretin hormone, it stimulates insulin release after a meal; however, in contrast to glucagon-like peptide-1 (GLP-1) it acts glucagonotropic at low blood glucose levels.[2,3] GIP also displays a bone-protective role as it both decreases bone resorption and increases bone formation.[4-8] In addition, the use of a GIP analogue has been shown to improve bone strength in ovariectomized mice.[9] The GIP receptor (GIPR) is a G protein-coupled receptor (GPCR) belonging to subclass B1 of the GPCR family.[10] In contrast to GLP-1, the glucose-lowering effect of GIP is impaired in patients with type 2 diabetes mellitus (T2DM), but the exact mechanism behind this remains to be described since the secretion of GIP seems normal or even elevated.[11-14] It has been hypothesized that the GIPR might be desensitized in the beta cells of patients with T2DM based on studies in diabetic rats,[15] but this remains to be proven in humans. Previously described differences between the rodent and human GIP system exemplifies the necessity for studies on the human GIPR.[16,17] Interestingly, it has been shown that the GIPR function in bone metabolism of patients with T2DM is not abolished,[18] which may point towards a cell, tissue and possibly species-specific down-regulation.

Owing to the impaired insulinotropic action of GIP in patients with T2DM,[11-14] the development of GIPR agonists has not been as successful as the development of GLP-1 receptor (GLP-1R) agonists.[19,20] In fact, it has been suggested[21] and also experimentally verified in rodents and non-human primates[22] that GIPR antagonists are useful in the treatment of T2DM and obesity possibly due to a resensitization of the GIP system and thereby phenocopying functional agonism. However, the GIP system is more complex in terms of pharmacological targeting. Thus, a recent phase 2 study demonstrated that a dual GIPR and GLP-1R agonist provided improved glucose control and weight loss than therapy with a GLP-1 agonist, suggesting that GIPR agonists may have a role in the treatment of T2DM and obesity (at least in combination with GLP-1R agonists).[23]

Several naturally occurring amino acid variants of the GIPR have been discovered in the human population.[24] The GIPR variant, [E354Q], is quite common with an allele frequency of 0.2.[25] It was described for the first time in 1998, where homozygous carriers of the variant were reported to have decreased levels in serum C-peptide concentrations (14% during fasting and 11% decrease after oral glucose tolerance test [OGTT]).[26] This was confirmed in another study, where homozygous carriers had slightly increased plasma glucose (0.15 mmol/L) 2 hours after glucose ingestion as well as lower insulin secretion after an OGTT.[27]

In contrast to the relatively weak effect on blood glucose, a stronger phenotype is observed in bone homeostasis as homozygous carriers of GIPR-[E354Q] have lower bone mineral density (BMD) and more than 50% increased fracture risk.[28] Several in vitro studies have been presented, yet with diverging results (summarized in Table 2). One study in Chinese hamster fibroblasts (CHL) revealed an increased cAMP accumulation for [E354Q].[26] Another study suggested decreased basal activity through $G_{\alpha s}$ in HEK293 cells,[24] whereas a third study presented no difference in cAMP accumulation between GIPR wt and [E354Q] upon expression in HEK293 cells[29] or CHO cells.[30] In addition, it has been reported that GIPR-[E354Q] have an increased GIP-induced desensitization caused by an impaired exocytosis of internalized receptors.[29] In the present study, we used in vitro and in silico methods to characterize GIPR-[E354Q] in terms of ligand-receptor binding kinetics and receptor-ligand interaction, signalling through different pathways and internalization pattern to determine whether any of these basic pharmacological properties could explain the altered phenotypes of persons homozygous for GIPR-[E354Q]. In broader terms, studies of GIPR variants may contribute to an enhanced understanding of the pharmacological potential of the GIP system and the mode-of-intervention for future drugs targeting the GIPR.

2 | MATERIALS AND METHODS

The study was conducted in accordance with the Basic & Clinical Pharmacology & Toxicology policy for experimental and clinical studies.[31]

2.1 | Materials

Human GIP(1-42) was purchased from Bachem, Bubendorf, Switzerland (H5645). cDNA of human GIPR wt and GIPR-[E354Q] were inserted in the pCMV-Tag2B vector. Human SNAP-GIPR was ordered and synthesized by Cisbio, Codolet, France, and inserted in pcDNA 3.1. SNAP-GIPR-[E354Q] was created by Quick Change Mutagenesis using the primers: GGTGTCCACCAGGTGGTGTTTGC (forward) and GCAAACACCACCTGGTGGACACC (reverse). The ^{125}I-labelled human GIP(1-42) was purchased from PerkinElmer, Skovlunde, Denmark (NEX402025UC). Tag-Lite SNAP-Lumi4-Tb was purchased from Cisbio, Codolet, France (SSNPTBX) and Fluorescein-O'-acetic acid from Sigma-Aldrich, Broendby, Denmark (88596-5MG-F).

2.2 | Transfection and tissue culture

COS-7 cells were cultured at 10% CO_2 and 37°C in Dulbecco's Modified Eagle Medium (DMEM) 1885 supplemented

with 10% foetal bovine serum (FBS), 2 mmol/L glutamine, 180 units/mL penicillin and 45 g/mL streptomycin. HEK293 cells were cultured at 10% CO_2 and 37°C in DMEM-GlutaMAX™-I supplemented with 10% FBS, 180 units/mL penicillin and 45 g/mL streptomycin. Both cell types were transfected using the calcium phosphate precipitation method.[32] Transiently transfected COS-7 cells were used in homologous competition binding, association and dissociation studies. Transiently transfected HEK293 cells were used for cAMP accumulation, β-arrestin 2 recruitment and real-time internalization experiments.

2.3 | Membrane preparation

Human GIPR wt, GIPR-[E354Q] and pcDNA3.1 membranes were prepared through several centrifugation steps of COS-7 cells expressing the corresponding receptor. The cells were scraped with PBS supplemented with a cOmplete™ protease inhibitor (Roche, Basel, Switzerland) and then homogenized using a Dounce. The homogenate was centrifuged for 3 minutes at 54 g (4°C), and subsequently, the supernatant of this homogenate was centrifuged for 45 minutes at 21 036 g at (4°C). The pellet was resuspended in storage buffer (20 mmol/L HEPES buffer (pH 7.2), 0.4 mmol/L $CaCl_2$, 2 mmol/L $MgCl_2$ and cOmplete™ protease inhibitor) and stored at −80°C. Protein determination was performed according to a standard Pierce™ BCA protein assay protocol (Thermo Scientific).

2.4 | Homologous competition binding assay

Transiently transfected COS-7 cells expressing either human GIPR wt or GIPR-[E354Q] were seeded in clear 96-well plates 1 day after transfection. The number of cells added per well was adjusted aiming for 5%-10% specific binding of ^{125}I-GIP(1-42). The next day, cells were assayed by competition binding for 3 hours at 4°C using ~15-40 pM of ^{125}I-GIP(1-42) and increasing concentrations of GIP(1-42) in binding buffer (50 mmol/L HEPES buffer, pH 7.2, supplemented with 0.5% bovine serum albumin [BSA]). After incubation, the cells were washed twice in ice-cold binding buffer and lysed using 200 mmol/L NaOH with 1% SDS for 30 minutes. The samples were analysed by the Wallac Wizard 1470 Gamma Counter.

2.5 | Radioligand association and dissociation assay

The association assay was executed by preparing a mixture of 30 μg human GIPR wt, GIPR-[E354Q] or pcDNA3.1 and 0.5 μg wheatgerm agglutinin-coated (WGA) PVT SPA beads (Perkin Elmer). This mixture was subsequently pre-coupled on a shaker in a total volume of 50 μL binding buffer (50 mmol/L HEPES buffer (pH 7.2), supplemented with

1 mmol/L $CaCl_2$, 5 mmol/L $MgCl_2$ and 0.5% (w/v) BSA) for 30 minutes at 30°C. The pre-coupling was followed by the distribution of membrane suspension in a CulturPlate-96 (Perkin Elmer, Groningen, The Netherlands) in a total volume of 90 μL binding buffer and spun down afterwards (1500 rpm, 5 minutes, RT). The reaction was initiated by the addition of ~42 pmol/L ^{125}I-GIP(1-42), and the amount of radioligand bound to receptor was measured every minute up to 100 minutes at 30°C using a TopCount NXT Microplate Scintillation & Luminescence Counter (Packard). For the dissociation experiment, the membrane suspension was distributed in a total volume of 85 μL binding buffer. The mixture was then pre-incubated for 100 minutes at 30°C with ^{125}I-GIP(1-42). The dissociation was initiated by adding 5 μL of 1 μmol/L unlabelled GIP(1-42). The amount of radioligand bound to receptor was measured every minute up to 999 minutes.

2.6 | cAMP and β-arrestin 2 assay

For the cAMP assay, HEK293 cells were transiently transfected with either GIPR wt or GIPR-[E354Q] and the bioluminescence resonance energy transfer (BRET) Epac-based sensor for cAMP, CAMYEL (cAMP sensor using YFP-Epac-RLuc).[33] For the β-arrestin 2 assay, HEK293 cells were transiently transfected with either GIPR wt or GIPR-[E354Q] and the donor Rluc8-Arrestin-3-Sp1, the acceptor mem-linker-citrine-SH3 and the GPCR kinase 2, GRK2 to facilitate β-arrestin 2 recruitment.[34] Two days following transfection, the cells were washed with PBS and resuspended in PBS with 5 mmol/L glucose. Then, 85 μL of the cell suspension solution was added to each well of a black-white 96-well isoplate followed by the addition of PBS with 5 μmol/L coelenterazine-h. Following a 10-minute. incubation, increasing concentrations of GIP(1-42) were added and incubated for an additional 30 minutes. Luminescence was measured by the Berthold Technologies Mithras Multilabel Reader (Rluc8 at 485 ± 40 nm and YFP at 530 ± 25 nm).

2.7 | Real-time internalization assay

The assay was performed as previously described.[35,36] In short, HEK293 cells transiently expressing the human SNAP-GIPR or SNAP-GIPR-[E354Q] were seeded in white 384-well plates the day after transfection at a density of 25 000 cells/well. The next day, the media was removed and SNAP-GIPR and SNAP-GIPR-[E354Q] were labelled with 100 nmol/L Tag-Lite SNAP-Lumi4-Tb (donor) in OptiMEM for 60 minutes at 37°C. Afterwards, the cells were washed with HBBS supplemented with internalization buffer (1 mmol/L $CaCl_2$, 1 mmol/L $MgCl_2$, 20 mmol/L HEPES and 0.1% Pluronic F-68, pH 7.4) followed by addition of 100 μmol/L pre-heated fluorescein-O'-acetic

acid (acceptor). The plate was placed in a 37°C incubator for 5 minutes prior to ligand addition to adjust the temperature. Then, the cells were stimulated with 37°C preheated human GIP(1-42) and internalization was measured every 3 minutes for 60 minutes at 37°C in PerkinElmer™ EnVision 2014 Multilabel Reader. The internalization data were corrected for any receptor expression differences by the ratio discrepancy between the two receptors.

2.8 | Molecular dynamics simulation of the GIPR

Since no crystal structures or cryo-EM structures of the full-length GIPR are available, a homology model of GIPR in complex with the naturally occurring agonist GIP(1-42) was made. This chimeric homology model was assembled using the cryo-EM structure of the activated GLP-1R [37] (residues 128-411, PDB: 5VAI, homology = 53%), the crystal structure of the extracellular domain of human GIPR [38] (*r* residues 29-122) and the NMR solution structure of GIP(1-42), [39] and missing residues 123-127 were taken from the GPCRdb.[40] Alignment of the receptor in the membrane was determined using the OPM database [41] after which the receptor was inserted in a hexagonal lipid bilayer using the CHARMM-GUI membrane builder consisting of 150 1-palmitoyl-2-oleoyl-sn-glycero-3-phosphocholine (POPC) lipids.[42] The receptor and membrane were dissolved in water with physiological salt concentration (0.15 mol/L) resulting in a system size of approximately 80k atoms with a x/y radius of 8.5 nm and a height of 13 nm. The system was equilibrated in a NPT ensemble at 310 K for 150 ns after which it was simulated for 600 ns using the same ensemble and temperature with GROMACS 2018.3

as the MD engine.[43] The CHARMM36m force field was employed with TIP3P water molecules and a van der Waals cut-off radius of 1.2 nm.[44] All data analysis was performed using GROMACS tools and home-made scripts. The wild-type snapshot in Figure 1 is taken from the MD simulation. The [E354Q] image is mutated using PyMol only to visualize that the mutation from glutamic acid to glutamine allows for preservation of the hydrogen bond interaction between the carbonyl and N-terminal nitrogen.

2.9 | Data and statistical analysis

Kinetic binding parameters and IC_{50} and EC_{50} values were determined by non-linear regression using GraphPad Prism 7 & 8. Sigmoid curves were fitted logistically with a Hill slope of 1 or −1 for the activation or binding curves, respectively. Internalization rates were determined by one-phase association analysis using GraphPad Prism 7. The observed rate constants K_{obs} (minute^{-1}) of ^{125}I-GIP(1-42) to GIPR wt and [E543Q] were obtained by plotting the data to a one-phase association model. The dissociation rate constants K_{off} (minute^{-1}) were acquired by plotting data to a two-phase decay model. The association rate constants for each phase $K_{on\ (phase)}$ (nmol/L^{-1} minute^{-1}) were calculated according to the following equation:

$$K_{on\ (phase)} = \frac{K_{obs} - K_{off\ (phase)}}{[L]}$$

In which [L] is the ligand concentration in nmol/L. To correct for the one-phase association, a single K_{on} (nmol/L^{-1} minute^{-1}) value, covering both phases of the dissociation rate ($K_{on\ (slow)}$ and $K_{on\ (fast)}$), was calculated as follows:

FIGURE 1 Illustration of GIPR wt and GIPR-[E354Q]. The mutation of GIPR-[E354Q] is located within the sixth transmembrane helix of the receptor. The genotype distribution among Europeans is 63% wild-type, 33% heterozygous and 4% homozygous[25]
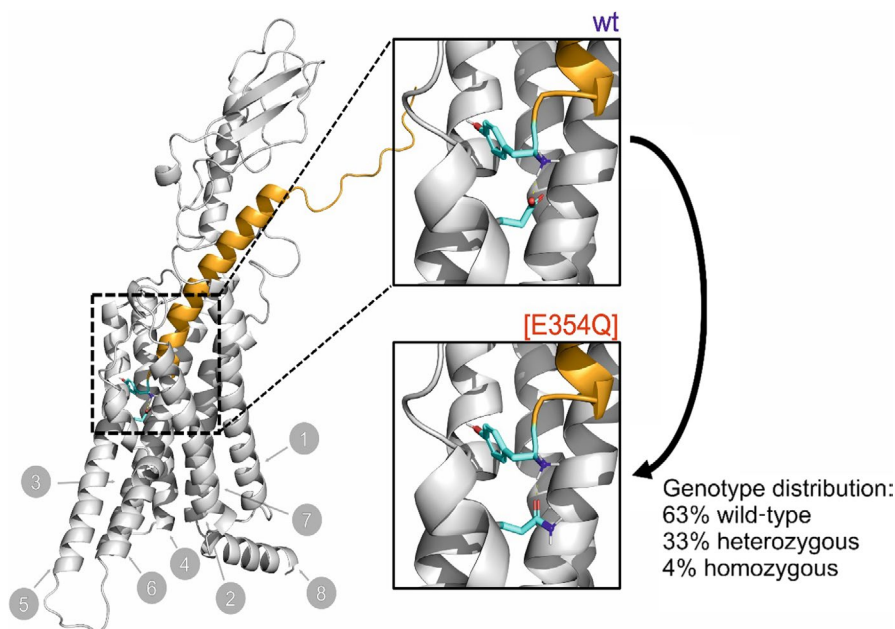
$$K_{on} = K_{on\ (fast)} * \%fast + K_{on\ (slow)} * \%slow$$

wherein %fast is the contribution of $K_{off\ (fast)}$ to the association rate constant and %slow is the contribution of $K_{off\ (slow)}$ to the association rate constant. The residence time (RT) in minutes was acquired as follows:

$$RT = \frac{1}{K_{off\ (phase)}}$$

EC_{50} and E_{max} values and binding parameters were compared by an unpaired Student t test. Internalization rates were compared by a one-way ANOVA with multiple comparisons. In both tests, $P < .05$ was considered significant different.

3 | RESULTS

The GIPR variant [E354Q] is quite common in the human population with the genotype distribution of 63% wt, 33% heterozygous carriers and 4% homozygous carriers.[25] It is located in the sixth transmembrane domain of the receptor close to the extracellular site (Figure 1). To gain understanding of where in the receptor E354 is situated and what its role is in ligand binding, we decided to employ molecular dynamic (MD) simulation to study the GIPR in complex with the endogenous agonist GIP(1-42). Hydrogen bond analysis of the MD simulations shows that the N-terminal nitrogen of GIP(1-42) forms a salt bridge with the carboxylic acid of E354 for approximately 78% of the simulated time indicating the importance of the interaction. The loss of the E354's anionic character upon mutation to a glutamine (Q) could perhaps weaken the interaction, but will still allow for a hydrogen bond in the same place, which might explain why previous studies described only little alteration in binding affinity.[24,26]

3.1 | Similar binding affinity but altered binding kinetics of GIP(1-42) on GIPR-[E354Q]

Inspired by the predicted slightly altered binding profile in [E354Q], we moved on with in vitro analyses of ligand binding and receptor activation. Homologous competition binding done at 4°C using ^{125}I-GIP(1-42) showed no difference in the affinity of GIP(1-42) to the GIPR wt and GIPR-[E354Q] with K_d of 2.39 ± 0.18 and 2.08 ± 0.12 nmol/L, respectively (Figure 2A, Table 1). Moreover, no difference was observed in the B_{max} values (Figure 2B). To determine whether the predicted altered binding mode in [E354Q] would change the binding kinetics, we measured association and dissociation rates of ^{125}I-GIP(1-42) using membranes from COS-7 cells expressing either of the receptors. The experiments were done at 30°C, and the kinetic profiles of the association of ^{125}I-GIP(1-42) were best fitted with a one-phase model
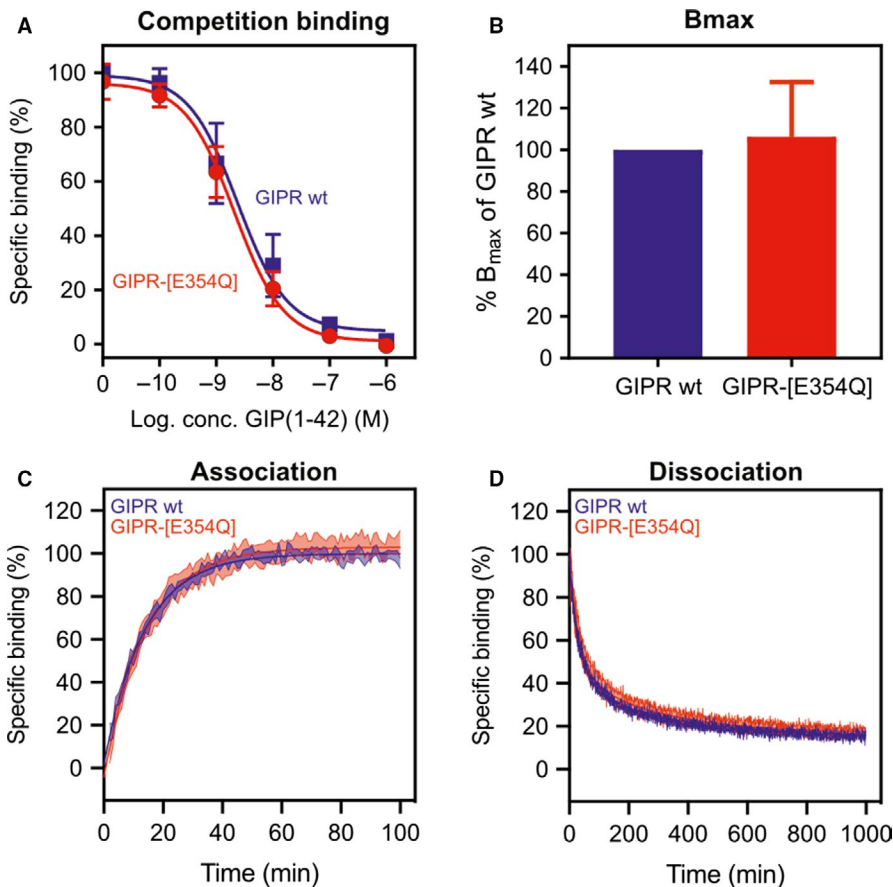

FIGURE 2 Binding affinity and kinetics of GIP(1-42) to GIPR wt and GIPR-[E354Q]. A, COS-7 cells were transiently transfected with human GIPR wt and GIPR-[E354Q] and assayed for homologous competition binding using ^{125}I-GIP(1-42) as radioligand and increasing concentrations of GIP(1-42). Data are normalized to the specific binding of the GIPR wt. B, The B_{max} value was calculated for both GIPR wt and GIPR-[E354Q] from the homologous competition binding data. For the association (C) and dissociation (D) experiments of ^{125}I-GIP(1-42), membranes of COS-7 cells expressing GIPR wt or GIPR-[E354Q] were used. Data are normalized to the specific binding of each receptor. Data are shown as mean ± SEM, n ≥ 3 independent experiments carried out in duplicates

TABLE 1 Binding parameters of ^{125}I-GIP(1-42) to GIPR wt and GIPR-[E354Q]

	GIPR wt	GIPR-[E354Q]
K_D (nmol/L)	2.39 ± 0.18	2.08 ± 0.12
K_{obs} (min^{-1})	$0.076 + 0.006$	0.073 ± 0.011
$K_{off\ (fast)}$ (min^{-1})	0.034 ± 0.006	0.030 ± 0.007
$K_{off\ (slow)}$ (min^{-1})	0.0044 ± 0.0001	0.0038 ± 0.0002
% fast phase	62 ± 2	64 ± 1
$RT_{(fast)}$ (min)	26.41 ± 0.74	$33.12 \pm 1.57*$
$RT_{(slow)}$ (min)	225.38 ± 3.12	$267.03 \pm 10.13*$
K_{on} (nM^{-1} * min^{-1})	1.283 ± 0.253	1.371 ± 0.378

Note: The residence times were compared by an unpaired Student t test ($*P < .05$).

with saturation reached after approximately 60 minutes for both receptors (Figure 2C). The observed on-rates (K_{obs}) for GIPR wt and GIPR-[E354Q] were 0.076 ± 0.006 and 0.073 ± 0.011 minute^{-1}, emphasizing that ^{125}I-GIP(1-42) binds with similar K_{obs} to both receptors. After obtained equilibrium, we could reverse the binding of ^{125}I-GIP(1-42) by the addition of 1 μmol/L unlabelled GIP(1-42), and the corresponding dissociation profiles were best fitted with a two-phase decay model with a fast and a slow phase (*%fast phase* 62% $\pm$ 2% and 64% $\pm$ 1%, respectively; Figure 2D). Interestingly, no complete dissociation of ^{125}I-GIP(1-42) was obtained, as a plateau was reached at approximately 15% remaining ^{125}I-GIP(1-42) binding on both receptors. As the off-rate was slower for GIPR-[E354Q], the residence time (*RT*; defined as the reciprocal value of K_{off}[45]) of ^{125}I-GIP(1-42) was higher than that of GIPR wt, both when calculated from the fast off-rate, $RT_{(fast)}$ 26.41 $\pm$ 0.74 versus 33.12 $\pm$ 1.57 min ($P = .018$), and from the slow off-rate $RT_{(slow)}$ 225.38 $\pm$ 3.12 versus 267.03 $\pm$ 10.13 min ($P = .017$; Table 1).

## 3.2 | GIPR-[E354Q] shows an increased cAMP signalling profile

Next, we studied whether GIPR-[E354Q] had a different signalling pattern compared with the GIPR wt. Several studies

have previously described diverging signalling profiles of GIPR wt and [E354Q].[24,26,29] We decided to use same cell type (HEK293 cells) and same signalling principle (BRET-based assays) to determine signalling via G protein-dependent and -independent pathways in order to avoid observational bias. Thus, we studied both cAMP accumulation and β-arrestin 2 recruitment in HEK293 cells expressing either GIPR wt or GIPR-[E354Q]. GIP(1-42) was found to be slightly more potent and efficacious in cAMP accumulation on GIPR-[E354Q] than GIPR wt with an EC_{50} of 0.34 $\pm$ 0.088 pmol/L compared with 0.69 $\pm$ 0.047 pmol/L and E_{max} of 137% $\pm$ 3.4% compared with 102% $\pm$ 1.7%, respectively (Figure 3A). In addition, GIPR-[E354Q] had a higher basal cAMP activity than GIPR wt reaching 17.5 $\pm$ 3.0% of E_{max} of GIPR wt. In contrast, no difference was observed in the ability of the receptors to recruit β-arrestin 2 with an EC_{50} of 5.5 $\pm$ 0.082 and 4.7 $\pm$ 0.23 nmol/L and E_{max} of 99% $\pm$ 3.3% and 97% $\pm$ 8.6%, respectively, upon addition of GIP(1-42) (Figure 3B).

3.3 | The GIPR-[E354Q] internalizes with a faster rate than GIPR wt

Due to the increased cAMP accumulation for GIPR-[E354Q], we went on and studied whether GIPR-[E354Q] had an altered internalization pattern. Again, we used HEK293 cells. In order to measure the internalization in real-time, we used SNAP-tagged versions of both receptors. Since internalization is very dependent on receptor expression,[36] the internalization data were corrected for any receptor expression differences measured by the donor signal. Both receptors were internalized after stimulation with 100 nmol/L and 1 μmol/L GIP(1-42) (Figure 4A-C); however, the GIPR-[E354Q] displayed faster internalization than GIPR wt at both 100 nmol/L and 1 μmol/L GIP(1-42) stimulation with the values of 0.086 $\pm$ 0.030 and 0.094 $\pm$ 0.011 compared with 0.037 $\pm$ 0.011 and 0.045 $\pm$ 0.006 minute^{-1}, respectively. Notably, no statistical significant differences were observed in the internalization efficacy between the two receptors ($_{bs}$AUC for 100 nmol/L GIP(1-42) stimulation: 61 $\pm$ 8.0 and 76 $\pm$ 45 for GIPR wt and GIPR-[E354Q], respectively, and

FIGURE 3 Human GIP(1-42) concentration curves for cAMP accumulation and β-arrestin 2 recruitment. HEK293 cells were transiently transfected with GIPR wt or GIPR-[E354Q] and (A) the Epac-based BRET sensor CAMYEL for cAMP accumulation or (B) the donor Rluc8-Arrestin-3-Sp1, the acceptor mem-linker-citrine-SH3 and the GPCR kinase 2 (GRK2) for β-arrestin 2 recruitment. Data are shown as mean $\pm$ SEM, n = 3 independent experiments carried out in duplicates
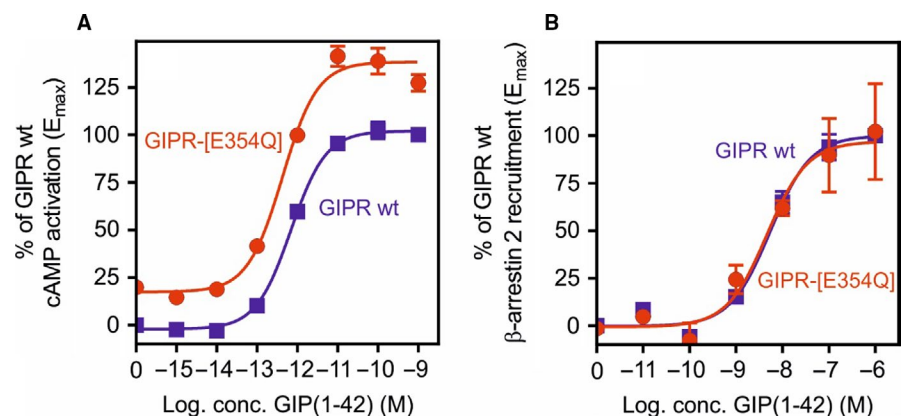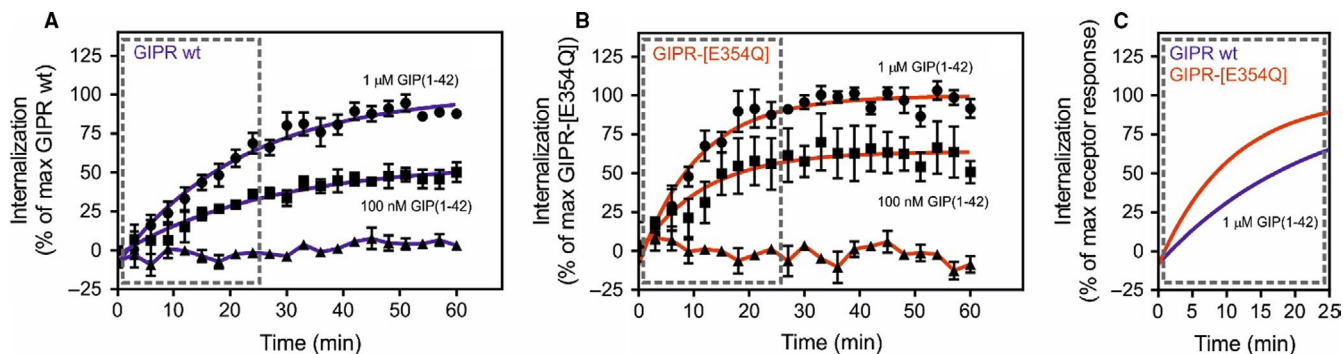
FIGURE 4 Internalization of SNAP-GIPR wt and SNAP-GIPR-[E354Q]. HEK293 cells were transiently transfected with SNAP-GIPR (A) or SNAP-GIPR-[E354Q] (B) and assayed for internalization over time following stimulation of 100 nmol/L (■) or 1 μmol/L (●) GIP(1-42). (C) A zoom of the first 25 min of internalization of SNAP-GIPR and SNAP-GIPR-[E354Q] following 1 μmol/L GIP(1-42) stimulation. Data are shown as mean ± SEM, n = 3 independent experiments carried out in triplicates

$_{bs}$AUC for 1 μmol/L GIP(1-42) stimulation: 97 ± 5.1 and 79 ± 55 for GIPR wt and GIPR-[E354Q], respectively).

4 | DISCUSSION

Our study demonstrates that the naturally occurring GIPR variant, [E354Q], that results in long-term impairment of the GIP system in humans and markedly increased fracture risk,[28] displays an altered molecular pharmacological phenotype compared with wt receptor. We find an enhanced internalization rate possibly explained by an altered ligand-binding mode, enhanced residence time and enhanced downstream signalling of the endogenous agonist GIP(1-42). Together with the previously described impaired recycling of [E354Q],[29] these findings suggest facilitated receptor desensitization and long-term down-regulation. This is highly relevant, as the GIP system seems more prone to desensitization as compared to the GLP-1 system given the decline in the insulinotropic action of GIP (but not of GLP-1) over time in patients with T2DM.[11-14] Thus, the phenotype of [E354Q] may represent the end-stage activity of the 'normal' wt GIP system in T2DM and obesity where hyperglycaemia and enhanced levels of GIP may have contributed to receptor desensitization.

4.1 | GIP(1-42) shows altered efficacy and residence time on GIPR-[E354Q]

The residence time, that is the time in which a drug remains bound to its target, has become increasingly acknowledged as an important parameter in pharmacology due to its strong predictive value for in vivo pharmacological activity.[45] The longer a certain drug occupies a receptor, the more profound effect is obtained, thus a higher efficacy may be reached.[46] This has for instance been shown for the β$_2$-adrenoceptor agonist, C26, having a longer residence time and higher potency and efficacy in several distinct signalling pathways compared with the endogenous agonist adrenaline.[47] Furthermore, it has been shown for three adenosine A$_1$ receptor (A$_1$R) agonists, all having similar affinity, but different binding kinetics, where the agonist (LUF6941) with the longest residence time had the greatest anti-lipolytic effect in rat adipocytes.[48] We found that GIP(1-42) bound with the same affinity to GIPR wt and GIPR-[E354Q] (Figure 2A). Looking further into the ligand-binding kinetics, no differences were observed in the association rates, but the dissociation was slower for GIP(1-42) on GIPR-[E5354Q], which in turn revealed a higher residence time for the agonist binding to the this receptor (Table 1). This aligns very well with the enhanced cAMP activity observed for GIPR-[E354Q] (Figure 3A), that, however, stands in contrast to a previous study describing the opposite (decreased cAMP) in HEK293 cells for GIPR-[E354Q].[24] This difference could be due to assay technicalities, as we used real-time cAMP measurements, whereas the luciferase reporter gene assay used in Ref[24] represents a downstream end-point cAMP measurement. Given the faster internalization of GIPR-[E354Q] (Figure 4B,C) and previously published decreased recycling leading to faster desensitization, it is likely that an end-point measurement will reveal overall lower activity levels for GIPR-[E354Q] as compared to wt receptor. Table 2 provides a comprehensive overview of our data of GIPR-[E354Q] in comparison with previously published data.

4.2 | High potency for agonist-induced cAMP accumulation relative to arrestin recruitment and affinity

Pharmacological characterizations of ligands for GPCRs include determination of affinity under equilibrium conditions (eg the IC_{50} value or K_D) and signalling activity (potency (EC_{50}) and efficacy (E_{max})).[45] We observed a huge preference towards G protein activation compared with arrestin recruitment with 8000- to 14 000-fold higher potency of

TABLE 2 Overview of in vitro results of GIPR-[E354Q] compared with GIPR wt

	Measurement														
	Binding			cAMP			Receptor surface expression			Internalization			Resensitization		
References	Cell type	Assay type	Result	Cell type	Assay type	Result	Cell type	Assay type	Result	Cell type	Assay type	Result	Cell type	Assay type	Result
Present study	HEK293	Ligand stimulation for 4 h at 4°C. Readout: 125I-GIP(1-42) binding	No difference in binding affinity of GIP(1-42)	HEK293	Ligand stimulation for 30 min. Readout: BRET luminescence	↑ basal and maximal activity and higher potency of [E354Q]	HEK293	Labelling of SNAP-tagged receptors. Readout: Donor signal	A tendency for ↓ expression of [E354Q] (data not shown)	HEK293	Ligand added just before measurement. Read out: Real-time FRET	↑ internalization rate of [E354Q]			
Fortin et al [24]	HEK293	Ligand stimulation for 8h at 4°C. Readout: 125I-GIP(1-42) binding	No difference in binding affinity of GIP(1-42)	HEK293	Ligand stimulation for 6 h. Readout: CRE-Luc luciferase	↓ basal and maximal activity	HEK293	Labelling of HA-tag. Readout: ELISA	↓ surface expression of [E354Q]						
Almind et al [26]	CHL	Ligand stimulation for 4h at 4°C. Readout: 125I-GIP(1-42) binding	No difference in binding affinity of GIP(1-42)	CHL	Ligand stimulation for 9 min. Readout: Intracellular tritiated cAMP	↓ basal activity but ↑ potency of [E354Q]									
Mohammad et al [29]				HEK293 3T3-L1 adipocytes	Ligand stimulation for 15 min. Readout: Immunoassay kit	No difference in activity	3T3-L1 adipocytes	Labelling of HA-tag. Readout: Immunofluorescence of fixed, non-permeabilized cells	No difference in expression	3T3-L1 adipocytes	Ligand stimulation for different time points. Readout: Anti-HA labelling of fixed cells	No difference in internalization rate	3T3-L1 adipocytes	Ligand stimulation for different time points. Readout: Anti-HA labelling of fixed cells	↓ exocytosis rate of [E354Q]
Kubota et al [30]				CHO	Ligand stimulation time not given. Readout: Radioimmunoassay kit	No difference in activity									

Note: The table displays an overview of our results and previously published in vitro results of GIPR-[E354Q]. Within each experiment, GIPR-[E354Q] is compared to GIPR wt.
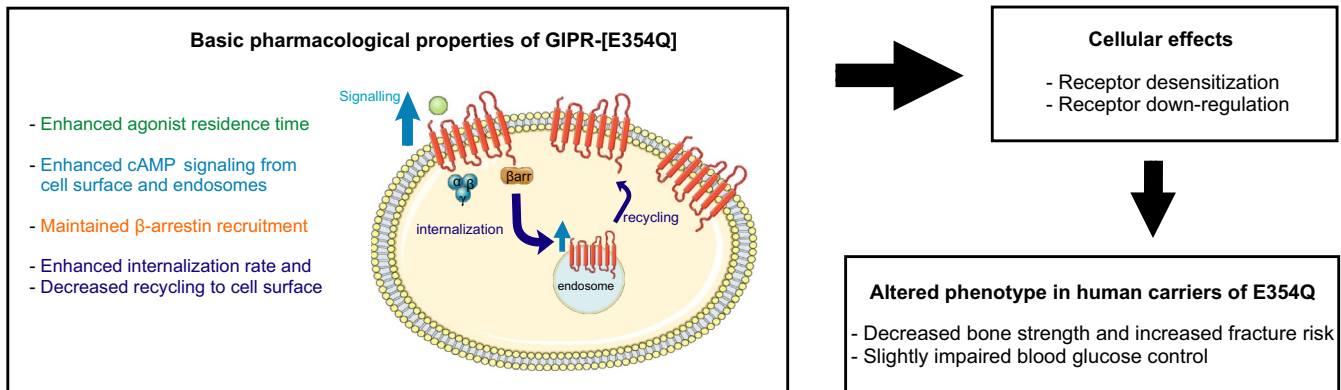
FIGURE 5 Illustration of altered signalling mechanism of GIPR-[E354Q] and possible link to long-term consequences

GIP(1-42)-induced cAMP accumulation in the two GIP receptors (Figure 3). This is in accordance with our previously published potency differences for the GIP receptor [35] and for the closely related GLP-1 receptor.[49,50] The same pattern was observed for the glucagon receptor (GCGR), though with a less pronounced difference.[49] A contributing factor to the higher potency observed for class B1 receptors to induce cAMP accumulation could be downstream amplification of $G_{\alpha s}$ which is not the case for β-arrestin recruitment and internalization. However, as other $G_{\alpha s}$-coupled receptors, such as class A receptors, like the adrenergic receptors do not display such bias towards $G_{\alpha s}$ over arrestin recruitment, it could also reflect that $G_{\alpha s}$ is the main signalling pathway during physiological control. A similar difference (3000-6000-fold) was observed when comparing the nanomolar binding affinity (K_D) to the picomolar potency (EC_{50}) in cAMP accumulation, again, a general tendency for ligands of class B GPCRs[51,52] and a phenomenon that ensures receptor signalling even with very little occupancy. This suggests the presence of spare receptors, that is a surplus of receptors relative to the occupancy needed for signalling output,[53] and could reflect the high importance of receptor signalling in human health (such as blood glucose regulation among other roles for the incretin receptors). It is, however, also likely that the downstream amplification of cAMP contributes to the potency:affinity difference.

4.3 | GIPR desensitization and signalling from endosomes

It is well known that the insulinotropic action of GIP is diminished in patients with T2DM[11-14]; however, the exact mechanism for this is not known. Maintained high plasma levels of GIP in patients with T2DM exclude lack of ligand to explain the diminished effect.[54] It has, however, been suggested that an increased GIPR desensitization in the beta cell could be involved in the impaired response of GIP to hyperglycaemia in patients with T2DM (as reported in diabetic rats[15]) or that downstream GIPR signalling is altered in the beta cells.[55] We have previously shown that the GIPR internalizes in a

low-potent, β-arrestin-dependent manner with equal importance of β-arrestin 1 and β-arrestin 2 and only minimum internalization in the absence of arrestins.[35] The low-potent internalization observed for GIPR and for other class B GPCRs thus aligns well with the low-potent β-arrestin recruitment for these receptors as observed in for instance the GLP-1R and the GCGR.[50,56] Here, we describe that the GIPR variant [E354Q] internalizes faster than the wt receptor (Figure 4B) possibly caused by altered agonist binding mode and kinetics with the increased residence time of the agonist (and a subsequent higher cAMP-mediated signalling which for the GIPR has been reported to also occur intracellularly from GIPR expressed in endosomes[57]). Together with the reported impaired exocytosis of GIPR-[E354Q],[29] the increased internalization will contribute to receptor desensitization and down-regulation over time (Figure 5). Thus, the impaired recovery of GIPR-[E354Q] may over time lead to an impaired response of GIP resulting in the altered bone homeostasis and blood glucose control in E354Q carriers. This resembles the suggested desensitization of the wt GIP system in patients with T2DM, and it can therefore be hypothesized that the increased desensitization of GIPR-[E354Q] mimics what happens over time in T2DM and that studies of the GIPR-[E354Q] signalling might contribute to a better understanding of the decreased sensitivity of the wt GIP system in T2DM.

CONFLICT OF INTEREST

MBNG, WJCvdV, SG, FXS, BH, HBO, and MMR declare that they have no conflict of interest.

REFERENCE

1. Baggio LL, Drucker DJ. Biology of Incretins: GLP-1 and GIP. *Gastroenterology*. 2007;132(6):2131-2157.

2. Christensen M, Calanna S, Sparre-Ulrich AH, et al. Glucose-dependent insulinotropic polypeptide augments glucagon responses to hypoglycemia in type 1 diabetes. *Diabetes*. 2015;64(1):72–78.

3. Christensen M, Vedtofte L, Holst JJ, Vilsboell T, Knop FK. Glucose-dependent insulinotropic polypeptide: a bifunctional glucose-dependent regulator of glucagon and insulin secretion in humans. *Diabetes*. 2011;60(12):3103-3109.

4. Nissen A, Christensen M, Knop FK, Vilsbøll T, Holst JJ, Hartmann B. Glucose-dependent insulinotropic polypeptide inhibits bone resorption in humans. *J Clin Endocrinol Metab*. 2014;99(11):E2325-E2329.

5. Bergmann NC, Lund AB, Heimbürger SM, et al. Mono- and Co-Activation of the GIP and GLP-1 Receptors Inhibits Bone Resorption. *Diabetes*. 2018;67(Supplement 1):1939-P.

6. Zhong Q, Itokawa T, Sridhar S, et al. Effects of glucose-dependent insulinotropic peptide on osteoclast function. *Am J Physiol Endocrinol Metab*. 2007;292:E543-E548.

7. Christensen MB, Lund A, Calanna S, et al. Glucose-dependent insulinotropic polypeptide (GIP) inhibits bone resorption independently of insulin and glycemia. *J Clin Endocrinol Metab*. 2018;103(1):288-294.

8. Skov-Jeppesen K, Svane MS, Martinussen C, et al. GLP-2 and GIP exert separate effects on bone turnover: a randomized, placebo-controlled, crossover study in healthy young men. *Bone*. 2019;125:178-185.

9. Mabilleau G, Gobron B, Mieczkowska A, Perrot R, Chappard D. Efficacy of targeting bone-specific GIP receptor in ovariectomy-induced bone loss. *J Endocrinol*. 2018;239:215-227.

10. Fredriksson R, Lagerstrom MC, Lundin LG, Schioth HB. The G-protein-coupled receptors in the human genome form five main families. Phylogenetic analysis, paralogon groups, and fingerprints. *Mol Pharmacol*. 2003;63(6):1256-1272.

11. Nauck MA, Heimesaat MM, Ørskov C, Holst JJ, Ebert R, Creutzfeldt W. Preserved incretin activity of glucagon-like peptide 1 [7-36 amide] but not of synthetic human gastric inhibitory polypeptide in patients with type-2 diabetes mellitus. *J Clin Investig*. 1993;91(1):301-307.

12. Meier JJ, Hucking K, Holst JJ, Deacon CF, Schmiegel WH, Nauck MA. Reduced insulinotropic effect of gastric inhibitory polypeptide in first-degree relatives of patients with type 2 diabetes. *Diabetes*. 2001;50(11):2497-2504.

13. Ross SA, Brown JC, Dupre J. Hypersecretion of gastric inhibitory polypeptide following oral glucose in diabetes mellitus. *Diabetes*. 1977;26(6):525-529.

14. Jones IR, Owens DR, Luzio S, Williams S, Hayes TM. The glucose dependent insulinotropic polypeptide response to oral glucose and mixed meals is increased in patients with type 2 (non-insulin-dependent) diabetes mellitus. *Diabetologia*. 1989;32(9):668-677.

15. Lynn FC, Pamir N, Ng EH, McIntosh CH, Kieffer TJ, Pederson RA. Defective glucose-dependent insulinotropic polypeptide receptor expression in diabetic fatty Zucker rats. *Diabetes*. 2001;50(5):1004-1011.

16. Sparre-Ulrich AH, Hansen LS, Svendsen B, et al. Species-specific action of (Pro3)GIP – A full agonist at human GIP receptors, but a partial agonist and competitive antagonist at rat and mouse GIP receptors. *Br J Pharmacol*. 2016;173(1):27-38.

17. Sparre-Ulrich AH, Gabe MN, Gasbjerg LS, et al. GIP(3–30)NH2 is a potent competitive antagonist of the GIP receptor and effectively inhibits GIP-mediated insulin, glucagon, and somatostatin release. *Biochem Pharmacol*. 2017;131:78-88.

18. Stensen S, Gasbjerg LS, Krogh LS, et al. 64-OR: postprandial effects of endogenous glucose-dependent insulinotropic polypeptide in type 2 diabetes. *Diabetes*. 2019;68(Supplement 1):64-OR.

19. Drucker DJ, Habener JF, Holst JJ. Discovery, characterization, and clinical development of the glucagon-like peptides. *J Clin Invest*. 2017;127(12):4217-4227.

20. Holst JJ. From the incretin concept and the discovery of GLP-1 to today's diabetes therapy. *Front Endocrinol (Lausanne)*. 2019;10:260.

21. Gasbjerg LS, Gabe M, Hartmann B, et al. Glucose-dependent insulinotropic polypeptide (GIP) receptor antagonists as anti-diabetic agents. *Peptides* 2018;100:173-181.

22. Killion EA, Wang J. Anti-obesity effects of GIPR antagonists alone and in combination with GLP-1R agonists in preclinical models. *Sci Transl Med*. 2018;10(472):eaat3392.

23. Frias JP, Nauck MA, Van J, et al. Efficacy and safety of LY3298176, a novel dual GIP and GLP-1 receptor agonist, in patients with type 2 diabetes: a randomised, placebo-controlled and active comparator-controlled phase 2 trial. *Lancet*. 2018;392(10160):2180-2193.

24. Fortin J-P, Schroeder JC, Zhu Y, Beinborn M, Kopin AS. Pharmacological characterization of human incretin receptor missense variants. *J Pharmacol Exp Ther*. 2010;332(1):274-280.

25. https://gnomad.broadinstitute.org/variant/19-46181392-G-C. Accessed April 26, 2019.

26. Almind K, Ambye L, Urhammer SA, et al. Discovery of amino acid variants in the human glucose-dependent insulinotropic polypeptide (GIP) receptor: the impact on the pancreatic beta cell responses and functional expression studies in Chinese hamster fibroblast cells. *Diabetologia*. 1998;41(10):1194-1198.

27. Saxena R, Hivert M-F, Langenberg C, et al. Genetic variation in GIPR influences the glucose and insulin responses to an oral glucose challenge. *Nat Genet*. 2010;42(2):142-148.

28. Torekov SS, Harsløf T, Rejnmark L, et al. A functional amino acid substitution in the Glucose-Dependent Insulinotropic Polypeptide Receptor (GIPR) gene is associated with lower bone mineral density and increased fracture risk. *J Clin Endocrinol Metab*. 2014;99(4):E729-E733.

29. Mohammad S, Patel RT, Bruno J, Panhwar MS, Wen J, McGraw TE. A naturally occurring gip receptor variant undergoes enhanced agonist-induced desensitization, which impairs GIP control of adipose insulin sensitivity. *Mol Cell Biol*. 2014;34(19):3618-3629.

30. Kubota A, Yamada Y, Hayami T, et al. Identification of two missense mutations in the GIP receptor gene: a functional study and association analysis with NIDDM: no evidence of association with Japanese NIDDM subjects. *Diabetes*. 1996;45(12):1701-1705.

31. Tveden-Nyborg P, Bergmann TK, Lykkesfeldt J. Basic & Clinical Pharmacology & Toxicology Policy for Experimental and Clinical studies. *Basic Clin Pharmacol Toxicol*. 2018;123(3):233-235.

32. Jensen PC, Thiele S, Ulven T, Schwartz TW, Rosenkilde MM. Positive versus negative modulation of different endogenous chemokines for CC-chemokine receptor 1 by small molecule agonists through allosteric versus orthosteric binding. *J Biol Chem*. 2008;283(34):23121-23128.

33. Jiang LI, Collins J, Davis R, et al. Use of a cAMP BRET sensor to characterize a novel regulation of cAMP by the sphingosine 1-phosphate/G13 pathway. *J Biol Chem.* 2007;282(14):10576-10584.

34. Donthamsetti P, Quejada JR, Javitch JA, Gurevich VV, Lambert NA. Using Bioluminescence Resonance Energy Transfer (BRET) to characterize agonist-induced arrestin recruitment to modified and unmodified G protein-coupled receptors. *Curr Protoc Pharmacol.* 2015;70(2):pp. 14.1-.

35. Gabe M, Sparre-Ulrich AH, Pedersen MF, et al. Human GIP(3–30) NH2 inhibits G protein-dependent as well as G protein-independent signaling and is selective for the GIP receptor with high-affinity binding to primate but not rodent GIP receptors. *Biochem Pharmacol.* 2018;150:97-107.

36. Foster SR, Bräuner-Osborne H. *Investigating Internalization and Intracellular Trafficking of GPCRs: New Techniques and Real-Time Experimental Approaches*. Handbook of experimental pharmacology, Vol. 245. Berlin Heidelberg: Springer; 2018:41-61.

37. Zhang Y, Sun B, Feng D, et al. Cryo-EM structure of the activated GLP-1 receptor in complex with a G protein. *Nature.* 2017; 546:248.

38. Parthier C, Kleinschmidt M, Neumann P, et al. structure of the incretin-bound extracellular domain of a G protein-coupled receptor. *Proc Natl Acad Sci USA.* 2007;104(35):13942-13947.

39. Alaña I, Malthouse J, O'Harte F, Hewage CM. The bioactive conformation of glucose-dependent insulinotropic polypeptide by NMR and CD spectroscopy. *Proteins: Struct, Funct, Bioinf.* 2007;68(1):92-99.

40. Pándy-Szekeres G, Munk C, Tsonkov TM, et al. GPCRdb in 2018: adding GPCR structure models and ligands. *Nucleic Acids Res.* 2018;46(D1):D440-D446.

41. Lomize MA, Pogozheva ID, Joo H, Mosberg HI, Lomize AL. OPM database and PPM web server: resources for positioning of proteins in membranes. *Nucleic Acids Res.* 2012;40(D1):D370-D376.

42. Wu EL, Cheng X, Jo S, et al. CHARMM-GUI Membrane Builder toward realistic biological membrane simulations. *J Comput Chem.* 2014;35(27):1997-2004.

43. Xu Z, Li D, Baohua J. Quantification of the stiffness and strength of cadherin ectodomain binding with different ions. *Theoretical Appl Mech Lett.* 2014;4(3):034001.

44. Huang J, Rauscher S, Nawrocki G, et al. CHARMM36m: an improved force field for folded and intrinsically disordered proteins. *Nat Methods.* 2017;14(1):71-73.

45. Copeland RA. The drug-target residence time model: a 10-year retrospective. *Nat Rev Drug Discovery.* 2016;15(2):87-95.

46. Guo D, Hillger JM, IJzerman AP, Heitman LH. Drug-target residence time–a case for G protein-coupled receptors. *Med Res Rev.* 2014;34(4):856-892.

47. Rosethorne EM, Bradley ME, Gherbi K, et al. Long receptor residence time of C26 contributes to super agonist activity at the human β2 ADrenoceptor. *Mol Pharmacol.* 2016;89(4):467-475.

48. Yun YI, Chen J, Liu R, et al. Long residence time adenosine A1 receptor agonists produce sustained wash-resistant antilipolytic effect in rat adipocytes. *Biochem Pharmacol.* 2019;164:45-52.

49. Jorgensen R, Kubale V, Vrecl M, Schwartz TW, Elling CE. Oxyntomodulin Differentially Affects Glucagon-Like Peptide-1 Receptor β-Arrestin Recruitment and Signaling through Gα. *J Pharmacol Exp Ther.* 2007;322(1):148-154.

50. Roed SN, Nøhr AC, Wismann P, et al. Functional consequences of glucagon-like peptide-1 receptor cross-talk and trafficking. *J Biol Chem.* 2015;290(2):1233-1243.

51. Svendsen B, Larsen O, Gabe M, et al. Insulin secretion depends on intra-islet glucagon signaling. *Cell Rep.* 2018;25(5):1127-1134.e2.

52. Hansen LS, Sparre-Ulrich AH, Christensen M, et al. N-terminally and C-terminally truncated forms of glucose-dependent insulinotropic polypeptide are high-affinity competitive antagonists of the human GIP receptor. *Br J Pharmacol.* 2016;173(5):826-838.

53. Neubig RR, Spedding M, Kenakin T, Christopoulos A. International union of pharmacology committee on receptor nomenclature and drug classification. XXXVIII. Update on terms and symbols in quantitative pharmacology. *Pharmacol Rev.* 2003;55(4):597-606.

54. Calanna S, Christensen M, Holst JJ, et al. Secretion of glucose-dependent insulinotropic polypeptide in patients with type 2 diabetes: systematic review and meta-analysis of clinical studies. *Diabetes Care.* 2013;36(10):3346-3352.

55. Meier JJ, Nauck MA. Is the diminished incretin effect in type 2 diabetes just an epi-phenomenon of impaired beta-cell function? *Diabetes.* 2010;59(5):1117-1125.

56. Roed SN, Wismann P, Underwood CR, et al. Real-time trafficking and signaling of the glucagon-like peptide-1 receptor. *Mol Cell Endocrinol.* 2014;382(2):938-949.

57. Ismail S, Gherardi M-J, Froese A, et al. Internalized Receptor for Glucose-dependent Insulinotropic Peptide stimulates adenylyl cyclase on early endosomes. *Biochem Pharmacol.* 2016;120:33-45.